OBSERVATION OF INDIGENOUS POLYCYCLIC AROMATIC HYDROCARBONS IN 'GIANT' CARBONACEOUS ANTARCTIC MICROMETEORITES

S. J. CLEMETT[1], X. D. F. CHILLIER[1], S. GILLETTE[1], R. N. ZARE[1], M. MAURETTE[2], C. ENGRAND[2,3] and G. KURAT[3]

[1] *Department of Chemistry, Stanford University, Stanford, CA 94305-5080, U.S.A.;* [2] *C.S.N.S.M., Batiment 104, 91405 Orsay-Campus, France;* [3] *Mineralogische Abteilung, Naturhistorisches Museum, Postfach 417, Vienna, Austria*

(Received 2 December, 1996)

Abstract. Two-step laser desorption/laser ionization mass spectrometry (μL^2MS) was used to establish the nature and mass distribution of polycyclic aromatic hydrocarbons (PAHs) in fragments of fifteen 'giant' ($\sim$200 μm) carbonaceous Antarctic micrometeorites (AMMs). Detectable concentrations of PAHs were observed in all AMMs showing a fine-grained matrix. The range of integrated PAH signal intensities varied between samples by over two orders of magnitude. No evidence of contamination whilst in the Antarctic environment could be found. The dramatic variation of both PAH signal intensities and mass distributions between AMMs along with comprehensive contamination checks demonstrates that particles are not exposed to terrestrial PAHs at or above detection limits, either subsequent, during or prior to collection. Comparison of the observed PAH distributions with those measured in three carbonaceous chondrites [Orgueil (CI1), Murchison (CM2) and Allende (CV3)] under identical conditions demonstrated that marked differences exist in the trace organic composition of these two sources of extraterrestrial matter. In general, AMMs show a far richer distribution of unalkylated 'parent' PAHs with more extended alkylation series (replacement of -H with -$(CH_2)_n$-H; n = 1, 2, 3 . . .). The degree of alkylation loosely correlates with a metamorphic index that represents the extent of frictional heating incurred during atmospheric entry. A search for possible effects of the chemical composition of the fine-grain matrix of host particles on the observed PAH distributions reveals that high degrees of alkylation are associated with high Na/Si ratios. These results, in addition to other observations by Maurette, indicate that 'giant' micrometeorites survive hypervelocity ($\geq$11 km s^{-1}) atmospheric entry unexpectedly well. Because such micrometeorites are believed to represent the dominant mass fraction of extraterrestrial material accreted by the Earth, they may have played a significant role in the prebiotic chemical evolution of the early Earth through the delivery of complex organic matter to the surface of the planet.

1. Introduction

The μL^2MS technique (see Section 2.2) has previously been used to analyze PAHs in a wide variety of extraterrestrial material captured by the Earth, including meteorites [1–4] and their acid residues [5], interplanetary dust particles (IDPs) [6,7], and interstellar graphite grains [8]. The results of these studies have been used to investigate a variety of cosmochemical processes such as thermal metamorphism and aqueous alteration in meteorite parent bodies; the characterization of the insoluble 'kerogen-like' matter constituting the bulk of the carbonaceous matter in carbonaceous chondrites; and the molecule specific isotopic characterization of PAHs in interstellar graphite grains extracted in the acid dissolution of primitive ordinary and carbonaceous chondrites.

Origins of Life and Evolution of the Biosphere **28:** 425–448, 1998.

Since July 1984, 'giant' micrometeorites (50–500 μm) captured by the Earth have been successfully collected in large numbers ($>10^5$) on both the Greenland and Antarctica ice sheets. Such micrometeorites appear to survive hypervelocity impact with the Earth's atmosphere surprisingly well, a result in disagreement with theoretical models proposed since the early work of Whipple [9,10] that suggest the probability of survival against melting for a 100 μm particle which is $\sim$400 times smaller than the experimentally observed value [11].

The 'cleanest' micrometeorites, those collected in Antarctica (AMMs), are mostly fine-grained carbonaceous objects that appear mineralogically similar to a relatively rare class of primitive meteorites known as carbonaceous chondrites ($\sim$4% of observed meteorite falls). From previous studies it is known that these micrometeorites contain high concentrations of carbonaceous material, with an average C content $\sim$8 wt. % [12].

We discuss below the extension of our investigation of PAHs in extraterrestrial material to include fragments of 'giant' AMMs which comprise the dominant mass fraction of extraterrestrial material accreted by the Earth [13–16]. Fifteen micrometeorites, chosen as a representative sampling, were selected for detailed analysis. Twelve of the AMMs were mineralogically similar to CM-type carbonaceous chondrites and represent the prevalent class of AMM. Each was ranked on a thermal metamorphism scale signifying the extent of frictional heating incurred during atmospheric entry. Additionally three other AMMs representing the rarer non-CM-type material were also studied. We have attempted to correlate PAH mass spectra from each particle to its thermal metamorphism index, and/or both the major and minor element composition of the fine grained matrix. Finally, we compare PAH distributions in AMMs to those of carbonaceous meteorites and discuss some of the preliminary implications and future prospects for continued PAH studies of this class of extraterrestrial material.

This paper is one in a series of three companion papers primarily intended to present an up to date discussion of the C chemistry of AMMs, and its implications in the fields of planetology and exobiology. The two other papers deal respectively with the search for amino acids in five distinct aliquots of about 35 micrometeorites each [17], and with the possible role of individual micrometeorites, considered as microscopic 'chondritic chemical reactors', in the synthesis of prebiotic molecules on the early Earth some four billion years ago [11,13,18].

2. Experimental

2.1. Antarctic micrometeorites: From collection to classification

The study of the C chemistry of micrometeorites is considerably more difficult than for meteorites as a consequence both of their small masses ($\sim 10^{-7}$–10^{-4} g) and the ease by which they can become contaminated, owing to their high surface-to-volume ratio, porosity, and chemical reactivity under prolonged exposure to gases

and water. Hence, all steps in micrometeorite studies must be carefully controlled from their collection in the cleanest, most unpolluted spots on the Earth (e.g., pre-industrial Antarctic ices) through to their selection and curation.

The cleanest collection of micrometeorites has been recovered from blue ice fields near Cap-Prudhomme about two kilometers from the margin of the Antarctica ice sheet during the summer of 1994. The heaviest snow falls ever recorded since 1950 combined with the effect of ultra-clean winds that blow almost constantly from the center to the margin of the ice sheet have helped to shield the blue ice fields from anthropogenic contamination. Moreover, a new 'micrometeorite factory' was designed to greatly reduce contamination of the ultraclean ice during collection. Potential problems include fly ash, rust particles, fuel spills 'sticking to the shoes', and trace material from plasticizers used in plastic tubing [19]. Particularly, in the new factory, all equipment exposed to the hot water used to melt the ice was made of either stainless steel or Teflon. This considerably reduced the potential contact of AMMs with contaminants during their 8 hr exposure in the 3–5 m^3 pocket of melt ice water from which they are recovered. In this study we have used AMMs selected exclusively from this collection.

AMMs are preserved subsequent to collection by deep freezing in a small aliquot of their original melt ice water, either in a Teflon vial (a favorite choice of inorganic geochemists) or a glass vial (a favorite choice of organic geochemists). The vial is then wrapped in a Teflon bag while in the field. During curation, aliquots are melted in a dust free room and dried on a stack of ash-free filters.

A pre-selection of $\sim$100 particles is initially made using a low magnification stereo-microscope, relying on simple selection criteria such as color ('dark' without any red discoloration) and texture (irregular shape with no euhedral surfaces). Typically up to 80% of particles selected using these criteria turn out to be AMMs. Next, each particle is broken into several subfragments using stainless steel tools, and one fragment of each particle is mounted as a polished section and analyzed with a scanning electron microscope (SEM) equipped with an energy dispersive x-ray spectrometer (EDS). Particles are identified as extraterrestrial based on a 'chondritic' composition of the non volatile elements, and on major textural features. The chondritic particles are then analyzed with an electron microprobe to allow accurate determination of their composition in both major and minor elements, which permits identification of specific mineral phases. The same section can be further analyzed by ion microprobe for isotopic composition.

From the results of these studies 'representative' AMMs can be selected for measurement of PAHs using the μL^2MS technique. In this case, a second fragment of each AMM is crushed onto a clean Au foil held between two fused quartz disks using a micro-crushing device similar to that used in the preparation of IDPs [6]. Remaining fragments are kept under a dry nitrogen atmosphere for future studies.

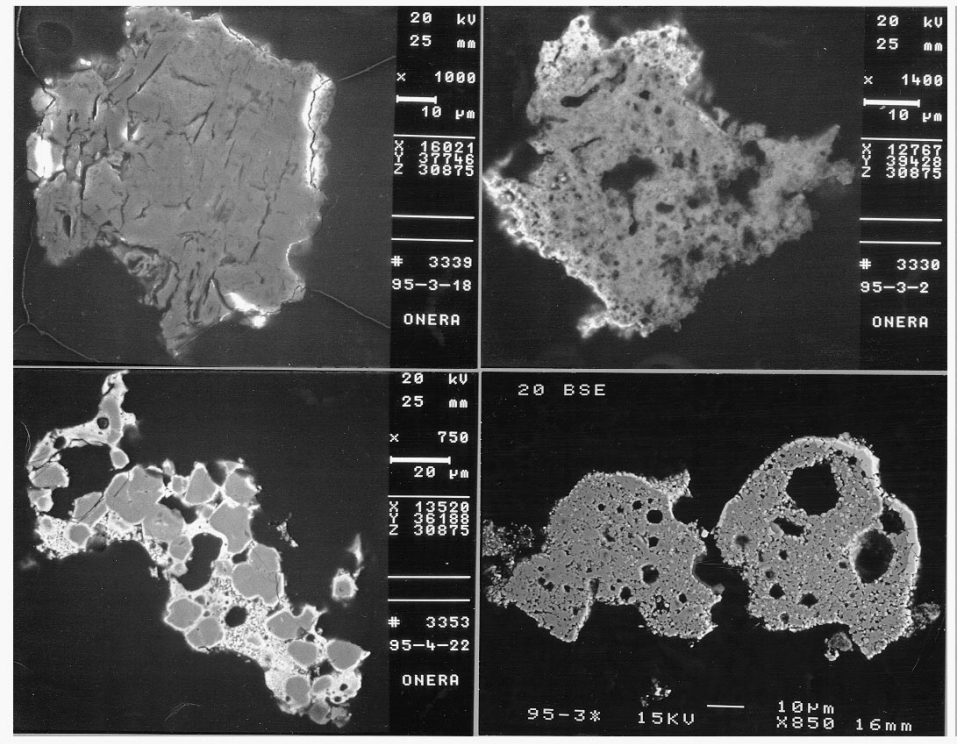

Figure 1a. Scanning electron microscope images of polished sections of four AMMs analyzed in this work. These particles belong to the dominant group of micrometeorites which are related to the CM chondrities and show a relatively low degree of PAH alkylation. They have been arranged on a scale of increasing thermal metamorphism, starting from top-left to and ending bottom-right: 95-3-18 is a fine-grained 'hydrous' micrometeorite that has experienced only minimal thermal metamorphism; 95-3-2 is a scoriaceous-type fine-grained micrometeorite showing a bright rind of vesicles, indicative of partial dehydration; 95-4-22 is a crystalline type micrometeorite composed mainly of anhydrous silicates (pyroxene and olivine – darker phases) embedded in a small fraction of fine-grained matrix (bright phase), which has been extensively dehydrated; 95-3-20 is a strongly heated scoriaceous-type micrometeorite, completely invaded by both tiny vesicles and magnetite crystals (bright spots), and which has almost been transformed into a 'melted' cosmic spherule.

2.2. THE μL^{2}MS INSTRUMENT

The technique of two-step laser mass spectrometry technique combines the advantages of laser desorption to volatilize intact neutral molecules from a solid sample with the molecular selectivity and sensitivity of resonance-enhanced multiphoton ionization (REMPI), and the high ion transmission, virtually unlimited mass range, and multichannel detection of a reflectron time-of-flight (RTOF) mass spectrometer.

In the first step, constituent molecules on the sample's surface are desorbed with a pulsed infrared laser beam focused to microscopic dimensions using a Cassegrainian microscope objective. The laser power is kept low to minimize

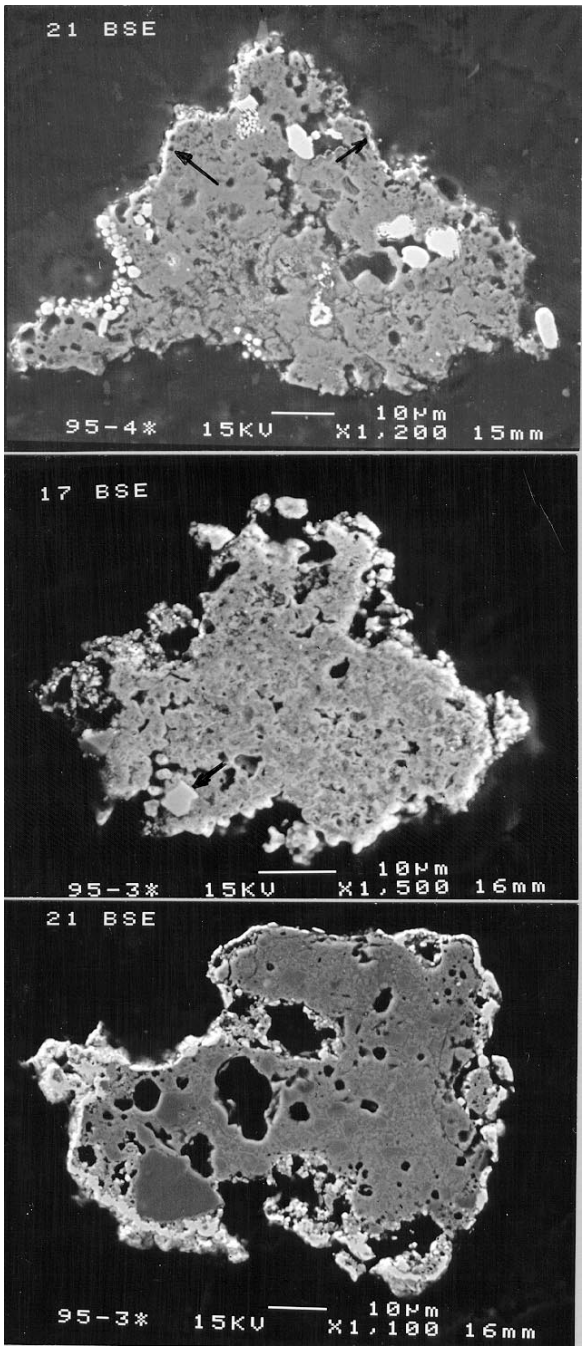

Figure 1b. Scanning electron microscope images of three polished sections of AMMs which show the highest degree of PAHs alkylation, and that mineralogically belong to relatively rare micrometeorite groups. They have been arranged on a scale of increasing thermal metamorphism from top to bottom: 95-4-21 is a fine-grained 'hydrous' micrometeorite, related to CI chondrites with a large concentration of magnetite framboids (bright phases), and shows few vesicles which are observed just below the bright thin magnetite rim (dark arrow); 95-3-17 is a fine grained micrometeorite containing small refractory inclusions (dark arrow) that have anomalous oxygen isotope composition; 95-3-21 is a fine grained micrometeorite with high contents of Na and Ca, that has been strongly heated.

decomposition and assure that only neutral species are desorbed. Pulsed laser desorption can, in a very short time span, deposit large quantities of energy into a highly localized area. Such processes provide a remarkably versatile method for introducing thermally labile and high molecular weight species intact into the gas phase. In the μL^2MS system, a CO_2 laser pulse (λ 10.6 μm; 150 ns FWHM) provides a heating rate of $\sim 10^8$ K s^{-1} [20].

In the second step, the desorbed molecules are ionized with a pulsed ultraviolet laser beam (λ 266 nm; 2.5 ns FWHM), and the resulting ions are extracted into a RTOF mass spectrometer. One of the main advantages of a photoionization process is that we can choose conditions that give rise to species-selective ionization. We presently use a (1+1) REMPI scheme, where absorption of one photon causes a molecule to make a transition to an electronically excited state ($S_0 \rightarrow S_1$) and absorption of a second photon causes ionization of that excited molecule. Wavelength selectivity results from the photon energy being resonant with a transition to an intermediate state. Because the ionization efficiency of a resonant mechanism is greater by many orders of magnitude than nonresonant multiphoton processes [21], only those molecules with a transition in resonance with the laser photon will be appreciably ionized. It is by virtue of this effect that we can achieve species-selective ionization. The chromophore we utilize is the benzene ring moiety which has strong absorption at 266 nm associated with electronic excitation of the aromatic ring ($\pi \rightarrow \pi*$). This chromophore provides an ionization window on PAHs. The real elegance of this ionization scheme lies not only in its selectivity, but also because it provides a very efficient 'soft ionization' route [22, 23]; that is, ions are formed with very little internal excitation and consequently do not undergo any appreciable fragmentation. The fact that intact molecules are detected is what makes the analysis of mixtures possible.

3. Results

3.1. Classification of Antarctic micrometeorites

After the preliminary SEM and EDS analyses a set of fifteen chondritic particles were selected for PAH analysis. This set included:

- Ten fine-grained particles belonging to the dominant family (>90% of particles) mineralogically related to the CM-type carbonaceous chondrites, and characterized by a highly unequilibrated assemblage of hydrous and anhydrous subgrains embedded in an abundant carbonaceous component, e.g., Figure 1a [95-3-18, 95-3-2 and 95-3-20].
- Two 'crystalline' particles composed of a few olivine and pyroxene crystals that are related to CM chondrites, e.g., Figure 1a [95-4-22].
- Three particles selected from three relatively rare families of AMMs related to CI chondrites ($\sim$5% of particles) and composed primarily of hydrous silicates

containing magnetite framboids, e.g., Figure 1b [95-4-21], or showing refractory inclusions with oxygen isotopic anomalies (∼2% of particles) and/or a high Na content (∼1% of the particles), e.g., Figure 1b [95-3-17 and 95-3-21].

The dominant CM-type particles were additionally selected to show a range of different degrees of 'invasion' by vesicles. Such vesicles are interpreted to be a result of the loss of water from hydrous silicate phases as a result of frictional heating incurred upon atmospheric entry, and can therefore be used to determine a thermal metamorphism index. Additionally other volatiles such as H_2 or S from decomposition of sulfides could be responsible for some vesicles as is for example observed in lunar agglutinates. The particle reported in Figure 1a [95-3-18], has experienced a minimum degree of thermal reprocessing and shows no vesicle 'invasion', such particles are considered unmelted. The particle in Figure 1a [95-3-2], characterized by a 10 μm thick rind of vesicles, has experienced strong heating, which is mostly limited to the edge of the particle. The particle reported in Figure 1a [95-3-20], is fully invaded by the vesicles and so has been severely heated and dehydrated, but not melted. The latter particles constitute a group referred to as scoriaceous particles ('scoria') and represent ∼60% of particles in a random selection of 200 μm sized particles.

The bulk average chemical composition, as determined by electron microprobe, of the fifteen AMMs selected for PAH analysis is illustrated in Figure 2 by a Si/Mg/Fe ternary diagram. In Section 4.3 element-to-silicon ratios inferred from these analyses are used to investigate possible correlations between the nature and distribution of PAHs observed from particles and the chemical composition of the fine-grained host matrix.

3.2. Characterization of the observed PAH distributions

The five dominant peaks observed in the PAH spectra of carbonaceous chondrites involve 2- to 5-ring aromatic molecules as illustrated in Figure 3. A potentially large number of structural isomers exist for a given mass peak, especially for larger polycyclic molecules. Using only a single laser ionization wavelength, μL^2MS is unable to distinguish between structural isomers. Nevertheless, different isomers have different photoionization cross sections and mass assignments are generally based on the most probable isomer. In the case of signals at 178 atomic mass units (amu) and 202 amu, the possible isomer combinations are phenanthrene/anthracene and pyrene/fluoranthene. At the photoionization wavelength used in this study, 266 nm, the μL^2MS instrument is 19 times more sensitive to phenanthrene than to anthracene and 23 times more sensitive to pyrene than to fluoranthene [24]. Hence, masses 178 and 202 are assigned as phenanthrene and pyrene. In the case of higher masses, more structural isomers exist and assignments are based on those PAHs known to have high cross sections from comparison with standards.

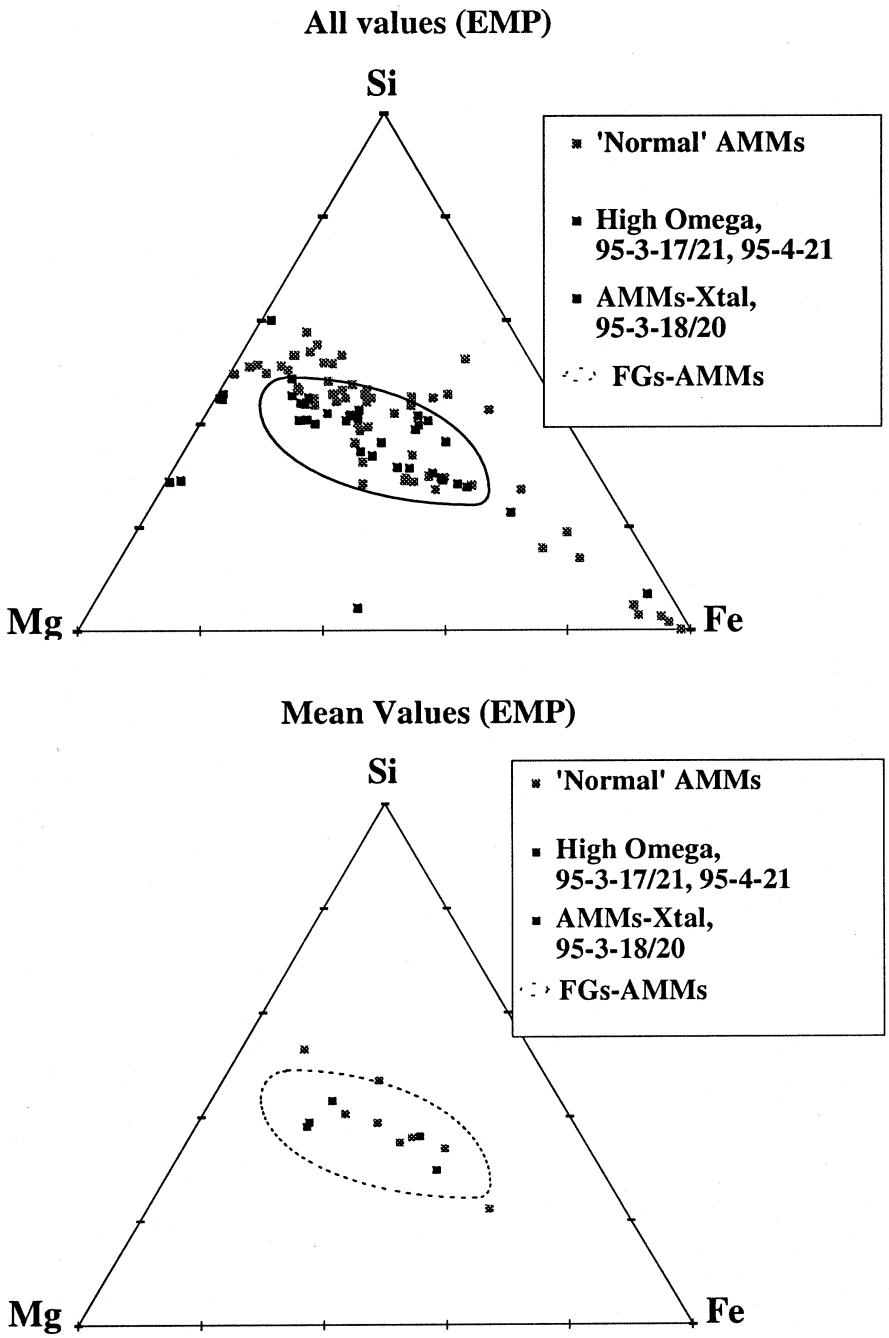

Figure 2. Ternary diagrams showing the results of accurate electron microprobe analyses, for the fifteen AMMs investigated in this work. The upper panel shows 'spot' analyses performed at several locations on each AMM, while the lower panel represents the average, bulk composition. The 'ellipsoidal' zone in the lower panel delineates the region of clustering from previous bulk analyses of ∼200 micrometeorites in the 50–400 μm size range that region defines 'chondritic' composition. All particles so far found on the Earth, satisfying both the requirement of being composed of aggregates of tiny subgrains and that have bulk 'chondritic composition', are extraterrestrial in origin.

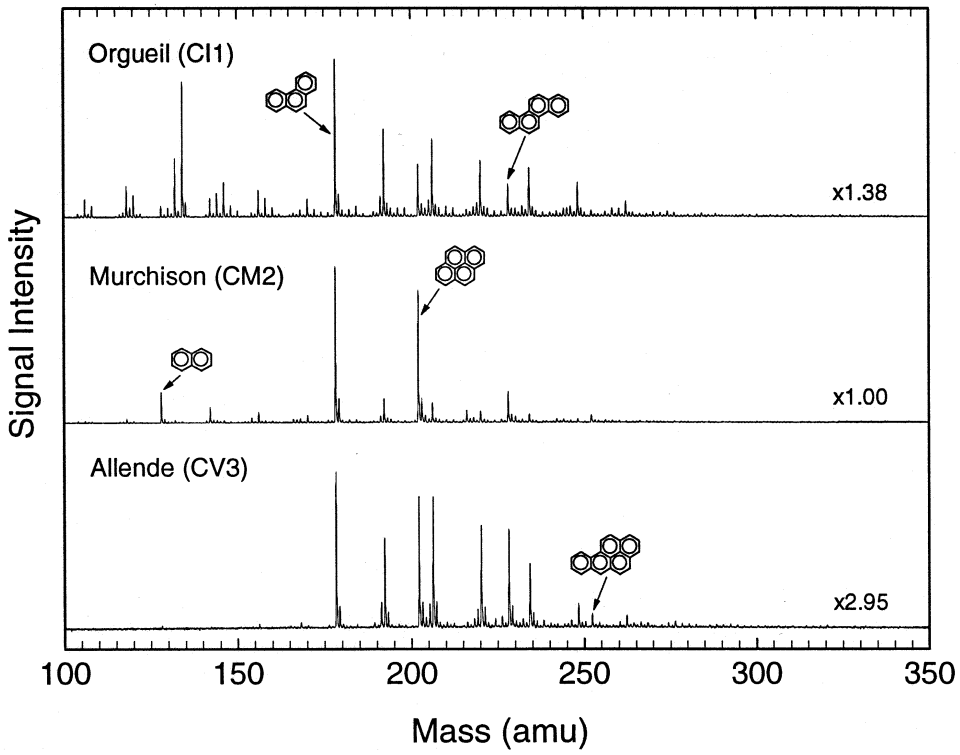

Figure 3. μL^2MS spectra of the three carbonaceous chondrites Orgueil (CI1), Murchison (CM2), and Allende (CV3). Each spectrum represents a 100-shot moving average on a individual matrix fragment of each meteorite. Relative scaling intensities between meteorites are indicated.

To characterize and compare complex PAH spectra we determine a set of parameters for each spectra that are independent of the strict structural isomer identification of a given peak. These parameters are:

- The desorption yield, γ, which represents the total integrated PAH signal from 100 to 350 amu. In this study, yields are defined relative to the AMM showing the strongest PAH signal.
- The extent of aromatization, which reflects the mass range of aromatic molecules observed.
- The index of alkylation, ξ, determined for parent PAH molecules that are common to both AMMs and carbonaceous chondrites.
- The abundance of vinyl-PAHs, AR-$(CH{=}CH)_n(CH_2)_m$-H (where AR refers to a parent PAH) relative to the saturated homologous PAHs, AR-$(CH_2)_n$-H.

The index of alkylation, ξ, for a given parent PAH at mass *m* is calculated from the expression

$$\xi = \frac{1}{I_m N} \sum_{n=1}^{n=x} I_{(m+14n)} n$$

where

N = the number of alkylatable positions on the parent PAH;
n = the number of C atoms in alkyl chain groups attached to the parent PAH;
x = the maximum number of C atoms observed in alkylation;
I_m = signal intensity of the parent PAH;
$I_{(m+14n)}$ = the signal intensity of the *n*th alkylated homolog.

When ξ is small, mass spectra are dominated by parent unalkylated PAHs; conversely when ξ is large, spectra are dominated by parent PAHs that show a complex higher mass distribution of alkylated homologs. In comparing meteorites and micrometeorites we first defined the ξ values for the PAHs observed to be common to both meteorite and micrometeorite PAH spectra, namely 178 amu (phenanthrene; $C_{14}H_{10}$), 202 amu (pyrene; $C_{16}H_{10}$) and 228 amu (chyrsene; $C_{20}H_{12}$), and then we defined a 'total' index of alkylation which is the sum of these values:

$$\xi_{\text{Total}} = \xi_{178\ amu} + \xi_{202\ amu} + \xi_{228\ amu}$$

Table I. Lists values of γ, ξ_{Total}, ξ_{178}, ξ_{202}, ξ_{252} for the thirteen carbonaceous AMMs studied as well as the carbonaceous chondrites, Murchison (CM2) and Allende (CV3).

3.3. PAHs IN CARBONACEOUS CHONDRITES

The three meteorites selected as standards in this study, Orgueil (CI1), Murchison (CM2) and Allende (CV3), are all carbonaceous chondrites characterized by a highly unequilibrated assemblage of hydrous and anhydrous minerals, including an abundant carbonaceous component with Orgueil (CI1) showing the highest C content ($\sim$3.5 wt. %). The meteorites differ with regard to:

- The hydrous mineral contents which are $\sim$99 wt. %, 50 wt %, and 0 wt. % respectively for Orgueil (CI1), Murchison (CM2), and Allende (CV3) (the driest) [25]. These values represent the extent of aqueous alteration incurred on the respective meteorite parent bodies.
- The degree of thermal metamorphism each meteorite suffered on its parent body. This temperature likely did not exceed 200 °C for Orgueil (CI1) and Murchison (CM2), whereas Allende (CV3) may have been heated as high as 600–700 °C [26].

Table I

Variation of the index of alkylation, ξ, and the integrated desorption yield γ, for the fifteen AMMs studied by μL^2MS ordered by increasing thermal metamorphism

Sample	ξ_{178}	ξ_{202}	ξ_{228}	ξ_{Total}	γ
Murchison (CM2)	0.015	0.049	0.000	0.064	
Allende (CV3)	0.170	0.140	0.000	0.310	
95-03-18	0.080	0.045	0.023	0.150	0.000044
95-04-21	0.650	0.078	0.000	0.720	0.250169
95-03-17	0.640	0.074	0.000	0.710	0.639693
95-03-11	0.217	0.068	0.000	0.290	1.000000
95-04-18	0.370	0.067	0.000	0.440	0.023998
95-03-24	0.350	0.048	0.033	0.430	0.100883
95-03-04	0.290	0.088	0.024	0.400	0.120788
95-03-21	0.380	0.340	0.110	0.830	0.040786
95-03-15	0.380	0.075	0.000	0.460	0.089236
95-04-11	0.450	0.026	0.000	0.480	0.28346
95-03-02	0.450	0.140	0.026	0.610	0.353062
95-04-25	0.330	0.028	0.000	0.360	0.208654
95-03-20	0.330	0.070	0.035	0.430	0.077077

In general, the meteoritic spectra appear similar to each other, Figure 3, and are characterized by their 'simplicity', particularly when compared to terrestrial particles rich in PAHs such as soot particles and soil samples. Five major parent PAHs are observed with only a weak alkylation series. Furthermore, no fragmentation products (peaks below 100 amu) or 'heavy' PAHs (peaks above 400 amu) can be discerned in the spectra. The dominant PAHs in Murchison (CM2) weigh 128 amu ($C_{10}H_8$; naphthalene), 178 amu ($C_{14}H_{10}$; phenanthrene), 202 amu ($C_{16}H_{10}$; pyrene), and 228 amu ($C_{18}H_{12}$; chrysene). Alklyated PAHs, e.g., 192 amu ($C_{14}H_9$-CH_2-H; methyl-phenanthrene) and 206 amu ($C_{14}H_{10}$-$(CH_2)_2$-H; dimethyl-phenanthrene), are less abundant. Orgueil (CI1) shows a qualitatively similar PAH distribution, whereas that of Allende (CV3) shows a more developed alkylation series.

Using Murchison (CM2) as the reference ($\gamma_{Murchison} \equiv 1$), the total PAH desorption yields decrease from Allende (CV3) ($\gamma = 0.60 \cdot \gamma_{Murchison}$) to Orgueil (CI1) ($\gamma = 0.58 \cdot \gamma_{Murchison}$). The values of the index of alkylation, ξ_{Total}, increases from Murchison (CM2) ($\xi_{Total} = 0.064$) to Allende ($\xi_{Total} = 0.310$).

3.4. PAHs IN ANTARCTIC MICROMETEORITES

Evidence for PAHs were observed in all fifteen AMMs studied, Figures 4a–d, though desorption yields varied by over two orders of magnitude between sam-

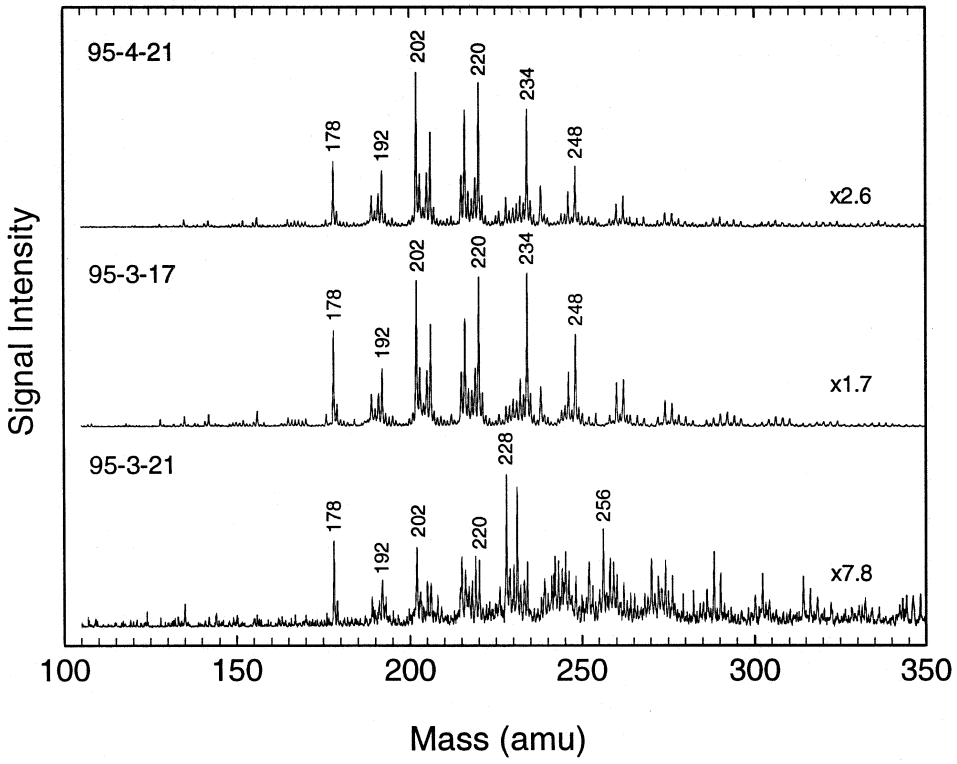

Figure 4. μL^2MS spectra of PAHs observed in the fifteen AMM studied. Figure 4a shows the spectra of the three particles with the highest index of alkylation; Figure 4b shows the two crystalline-type AMMs; while Figures 4c and 4d illustrate the spectra of the remaining ten AMMs that are all mineralogically related to CM-type chondrites.

ples. The suite of PAHs observed appear to be considerably more diverse than those of carbonaceous chondrites. Qualitatively they range from 'similar', e.g., Figure 4d [95-4-11], to vastly different, e.g., Figure 4d [95-3-20]. For carbonaceous chondrites the dominant PAH is phenanthrene ($C_{14}H_{10}$; 178 amu). Although phenanthrene is also strong in all the AMM spectra, it is never the dominant peak. For the AMMs the dominant PAHs observed are pyrene ($C_{16}H_{10}$; 202 amu) (7 particles), chrysene ($C_{18}H_{12}$; 228 amu) (6 particles), tetramethyl-phenanthrene ($C_{18}H_{18}$; 234 amu) (1 particle) and an unidentified PAH at 215 amu (fragment?) (1 particle). Typically, the individual peak intensities for the dominant PAHs in AMMs are much smaller (5–100 times) than observed in Murchison (CM2), but because the spectra of the AMMs show a more complex distribution of PAHs, the integrated desorption yields are comparable and in some cases greater than that of Murchison (CM2). The most significant difference between the PAHs observed in the carbonaceous chondrites and those in AMMs is the AMMs greater degree of alkylation, which is evident from the index of alkylation, ξ_{Total}, reported in Table I.

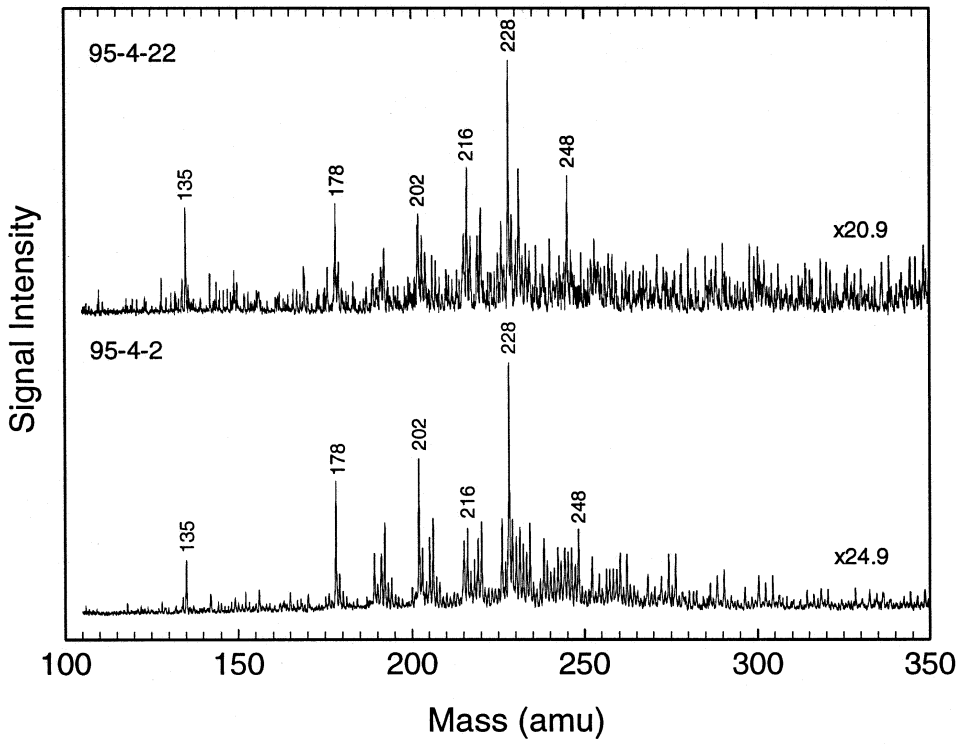

Figure 4b.

3.5. 'EXOTIC PAHS'

In addition to evidence for strong alkylation series in many of the AMM spectra extended peak series appear consistent with homologous series in which the alkyl substituents have undergone partial dehydrogenation, i.e., AR-$(CH{=}CH)_n(CH_2)_m$-H; where AR refers to a parent PAH. Such homologous series are generically described henceforth as vinyl-PAHs. Figure 5, illustrates the (alkyl -2H) phenanthrene series for particle 95-3-2. The presence of such vinyl-PAHs may promote interesting organo-metallic reactions. Brack [27] has noted that vinylic molecules such as ethylene can fix transition metals from the platinum group. The resulting 'Zeise' salt can be hydrolyzed in boiling water, yielding acetaldehyde, which generates the amino acid alanine in the presence of water and hydrogen cyanide. It will therefore be interesting to consider whether this type of reaction is also applicable to vinyl-PAHs.

No evidence was found for odd-mass PAHs with the exception of the strong peak at 215 amu observed on particle 95-3-2 illustrated in Figure 4d. In previous studies of IDPs collected in the stratosphere, two of the particles showed spectra

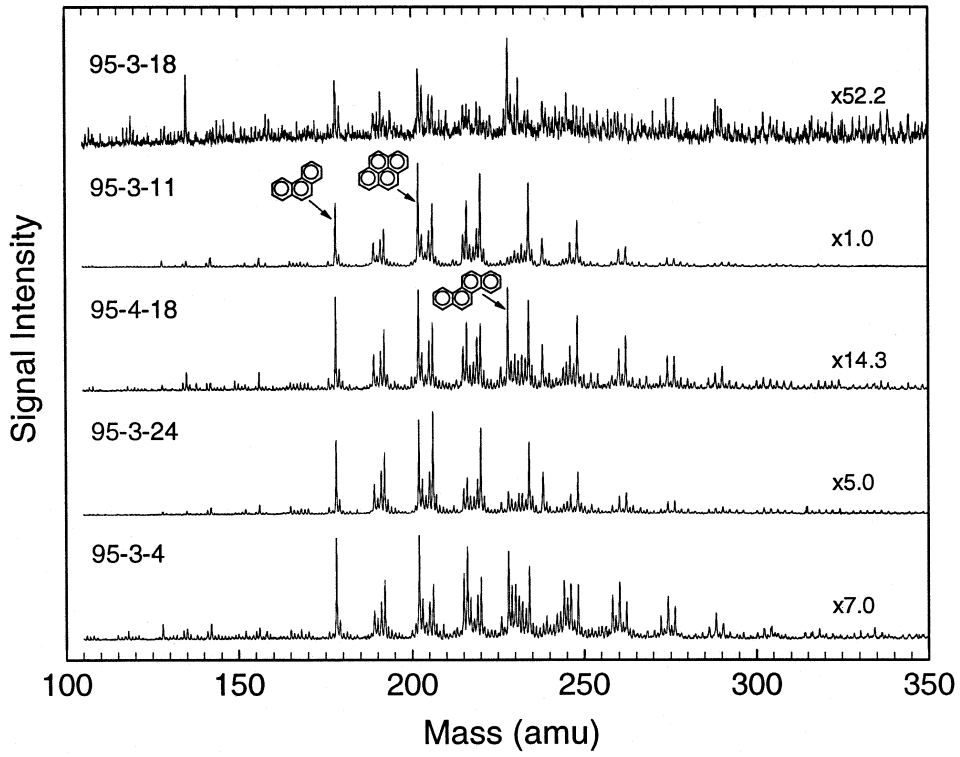

Figure 4c.

dominated by odd mass peaks interpreted to be caused by the presence of complex aromatic hydrocarbons with substituent groups containing nitrogen [6].

The mass resolution of the μL^{2}MS system under typical operating conditions is $\sim$1800, permitting clean ^{12}C/^{13}C molecular isotopic resolution of all PAH peaks not subject to chemical interferences. No evidence could be found for any molecules with a C isotope abundance differing significantly from Solar; the same observation was made for IDPs. These findings contrast with those of isotopically anomalous 'presolar' PAHs in interstellar graphite grains extracted from the acid-insoluble residue of the Murchison (CM2) meteorite [28].

4. Discussion

4.1. Arguments against terrestrial contamination

All AMMs analyzed in this work were collected from the field the *same* day, and from the *same* pocket of melt ice. After isolation they were stored in the *same* glass vial and handled in the *same* way under ultraclean conditions since the day of their collection. The wide disparity in the PAH spectra observed from these particles

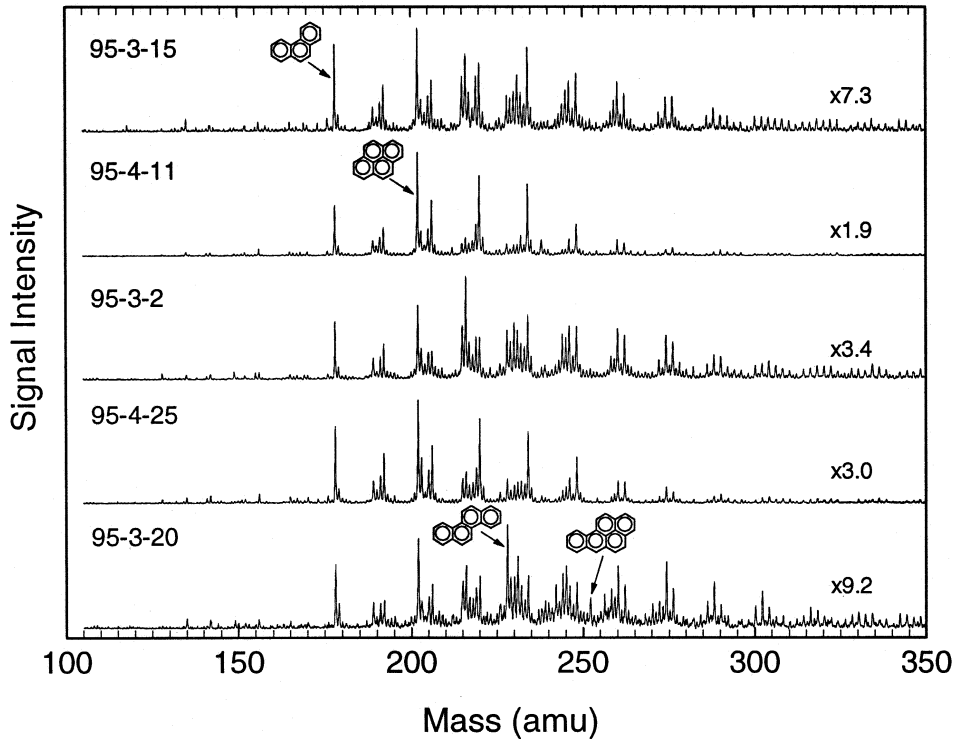

Figure 4d.

thus argues against a common contamination source. Additional arguments further support the extraterrestrial origin of the observed PAHs:

- In the most abundant CM-type AMMs the PAH spectra appear to show evidence of thermal alteration caused by atmospheric entry. This implies that PAHs must have been present prior to capture of the AMMs by the Earth.
- In spite of marked differences, the PAH spectra of the AMMs are still qualitatively similar to carbonaceous chondrites and certainly less complex than might be expected if their presence were from terrestrial contamination.
- In the 1991 collection of AMMs, the steam pipe used to melt the blue ice was made from steel and suffered from rust corrosion during operation. Small rust particles, initially formed as colloidal iron hydroxide, were thus simultaneously collected along with the AMMs. Such particles are morphologically identical to dark and fluffy AMMs, showing in particular a high surface area that presumably can efficiently trap contaminants from the melt water. Analysis of such rust particles show no PAHs within detection limits; see Figure 6.

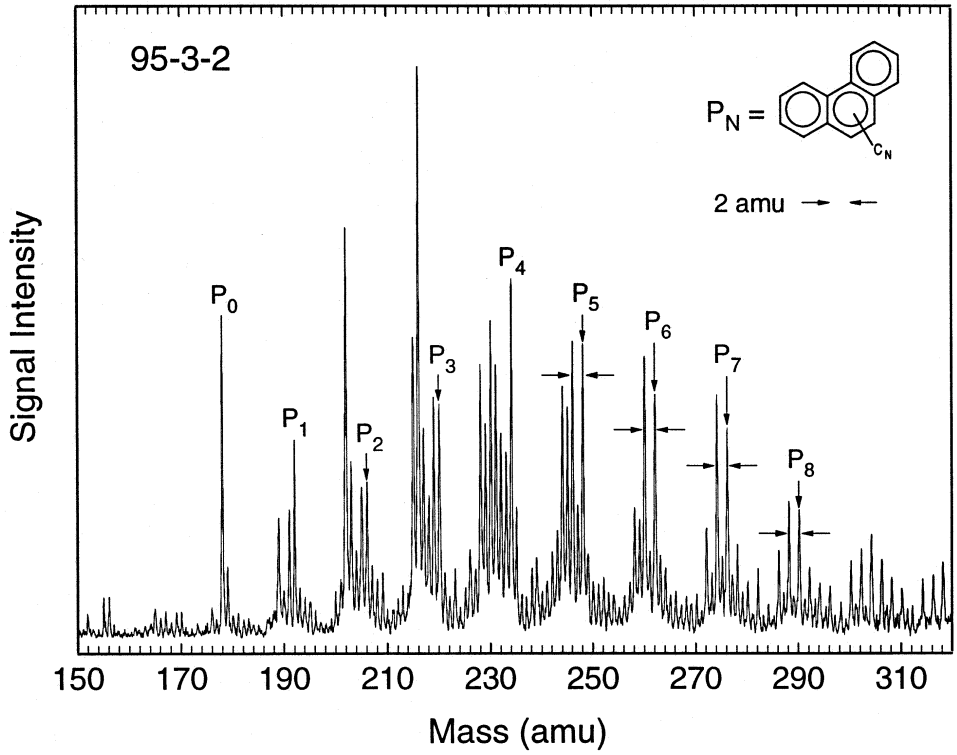

Figure 5. μL^2MS spectra of AMM 95-3-2 with an extended phenanthrene ($C_{14}H_{10}$; 178 amu) alkylation series which shows evidence of partial dehydrogenation that manifests itself as a well resolved alkyl -2H homologous series of vinyl-PAHs.

These observations imply that terrestrial PAH contamination introduced since the particles were trapped in the Antarctic ice is not significant. It might be argued that terrestrial contaminants were incorporated in and onto AMMs during gravitational settling in the atmosphere. In previous PAH studies of stratospherically collected IDPs, which owing to their smaller size ($\sim$10 μm) have a longer gravitational settling time, no evidence could be found to support the contention of atmospheric contamination [6]. It should be kept in mind though that other stratospheric contaminants, e.g., tiny deposits of acidic aerosols, are observed on the surface of some cosmic spherules which have had only minimal exposure to melt ice water [19].

4.2. INDEX OF ALKYLATION, PAH YIELDS, AND THERMAL METAMORPHISM

The nature and distribution of PAHs in meteorites reflect both their source within the early Solar System, and also their subsequent evolution. Meteorite classification seeks to recognize both of these factors.

The primary classification for chondritic meteorites leads to the identification of twelve chondrite classes (CI, CM, CO, CV, CR, CK, H, L, LL, R, EH and EL) that

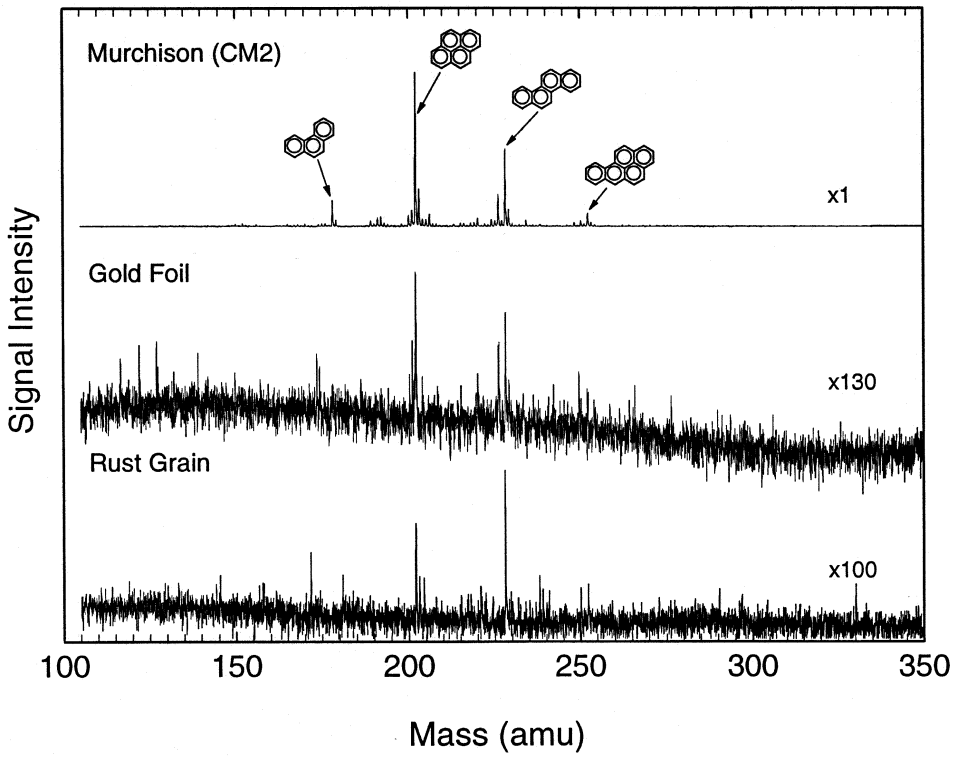

Figure 6. μL^2MS contamination spectra comparing the PAH distributions observed for Murchison (CM2) with a clean gold foil (on to which AMMs fragments were pressed prior to μL^2MS analysis) and a contaminant particle (rust particle – colloidal iron hydroxide) recovered with AMMs from the melt ice water.

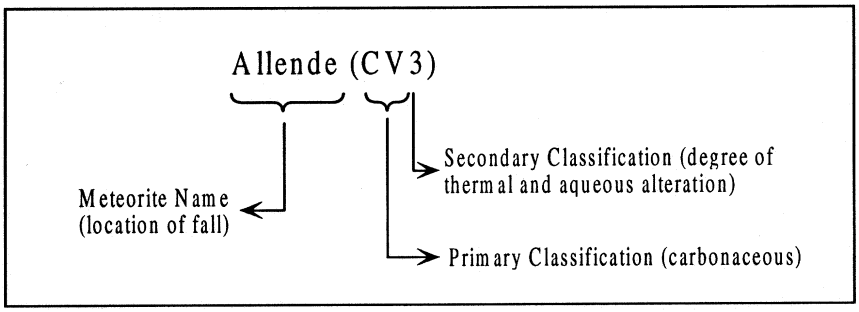

Scheme 1.

form the basis of the carbonaceous, ordinary, and enstatite chondrite groups. The secondary classification of chondrites attempts to describe the nature and extent of processes that occurred on the meteorite parent bodies after their accretion from the solar nebula. Four principal processes are recognized to have affected the

chondrites composition: thermal metamorphism; aqueous alteration; shock events; and brecciation.

The first two processes have received the most attention because they appear to show systematic variations from group to group. The extent of thermal metamorphism is counted upward starting at 3 and ending with 7, whereas aqueous alteration is counted downward starting with 3 (no alteration) and ending with 1 (fully altered). These numbers are appended to the primary chondrite classification [29,30]. Type 3 chondrites probably reflect the least altered and best preserved chondrites. Types 1 to 2 appeared to have been altered by hydrothermal processes, as evidenced in the conversion of anhydrous minerals, such as olivine, into clay-like minerals. Types 4 to 7 have been altered by thermal metamorphism, as evidenced by increasing recrystallization, which ultimately leads to the destruction of the chondritic texture in type 7. More recently, it has become evident that type 3 ordinary chondrites have experienced a considerable range of metamorphic intensity and thus type 3 ordinary chondrites are further subdivided into types 3.0-3.9, with type 3.3 representing the least altered material in regards to aqueous and thermal processing [31].

In Table I, four indexes of alkylation, ξ, are reported for the Murchison (CM2) and Allende (CV3) meteorites, corresponding to the alkylation series for the three dominant parent PAHs, ξ_{178}, ξ_{202}, ξ_{228}, and their sum, ξ_{Total}. Equivalent alkylation indexes are also reported for the thirteen carbonaceous AMMs analyzed. In previous work with meteoritic acid-insoluble residues, notable differences are observed in the carbonaceous and ordinary chondrites, reflecting both the degree of alkylation and the extent of aromatization [8]. Moreover, specific correlations are observed between the degree of alkylation and petrographic type even within a single chondrite class. In brief, higher degrees of alkylation, and a greater range of aromatization are observed in the more thermally metamorphosed chondrites. These observations support the hypothesis that the effects of secondary processing – thermal metamorphism and aqueous alteration – have played a significant role in shaping the organic content of these materials. Thus the composition of PAHs in such samples can act as an 'organic cosmothermometer' to track such processes. For the Murchison (CM2) and Allende (CV3) meteorite standards used in this study the total index of alkylation, increases from Murchison ($\xi_{\text{Total}} = 0.064$) to Allende ($\xi_{\text{Total}} = 0.310$) in agreement with the metamorphic (secondary) classifications of these meteorites. (It has also been shown that under laboratory-simulated thermal metamorphism studies the PAH distribution of Murchison (CM2) can be transformed to one similar to Allende (CV3) through extended heating at 873 K in an inert Ar atmosphere [8].)

For the fifteen AMMs studied we clearly see that most of the volatile PAHs, such as naphthalene ($C_{10}H_8$; 128 amu), are strongly depleted relative to either Murchison (CM2) or Allende (CV3). Even more striking, however, is the extent of alkylation which appears to be far higher than is observed within meteorites. These observations suggest that the AMMs have suffered extensive thermal metamor-

phism. Theoretical calculations of the frictional heating incurred by IDPs during their hypervelocity impact with the atmosphere predict that large IDPs approaching the size range of typical AMMs could not survive entry unmelted, i.e., they become cosmic spherules. Indeed, at a size of $\sim$100 μm, it is predicted that the ratio of unmelted AMMs to cosmic spherules is less than 0.1 (10%). This prediction was cited for a long time in the literature because of the apparent agreement with the observation of chondritic particles extracted from deep sea sediments by magnetic raking [16]. More recently it has become obvious that this observation is an artifact of the collection procedure. Theoretical predictions no longer support experimental observations [32], in the case of IDPs the observation of thermal gradients in particles suggest that effects such as endothermic phase transitions must also be considered when determining heating effects incurred during atmospheric entry [33].

Using data from the 1987, 1991 and 1994 collection of AMMs in the size range 50–100 μm, the ratio of unmelted AMMs to spherules was $\sim$4, i.e., about 400 times larger than predicted. Nevertheless, it is clear that all interplanetary particles with sizes in excess of $\sim$10 μm must have been heated to some extent during atmospheric entry, and this effect should increase with the size of the incoming particle [11].

In Section 3.1 it was noted that about half of AMMs collected from melt ice show small vesicles that invade the particle starting from the external surface. Recent ion microprobe studies allow determination of the amount of residual extraterrestrial water still locked within the constituent hydrous silicate phases [34]. Contrary to previous interpretations, these observations suggest that these vesicles do not reflect the onset of melting but rather the partial dehydration of phyllosilicates. Consequently, AMMs can be crudely ranked on a scale of increasing metamorphism, either by measuring the concentration of residual water, a complex procedure, or more simply by assessing the extent of vesicular invasion. On this 'metamorphic scale', particles range from truly unmelted (no vesicles; Figure 1a [95-3-18]), to partially dehydrated (vesicular rind; Figure 1a [95-3-2]), to strongly dehydrated (partially, Figure 1a [95-4-22], or completely invaded by vesicles and magnetite crystals, Figure 1a [95-3-20]).

In Figure 7 we report the variations of ξ values for AMMs showing a dominate fine-grained matrix and which have been sorted on a scale of increasing thermal metamorphism. At first glance these variations look uncorrelated with three particles (95-04-21, 95-03-17 and 95-03-21) showing very high ξ values; however, these three anomalous particles are mineralogically distinct from the other particles and are not members of the dominant CM-type of AMMs. If we consider just the CM-type AMMs then a rather smooth increase of ξ with thermal metamorphism is observed.

Because the least heated AMMs show a PAH distribution rather similar to that of carbonaceous chondrites, it seems likely that these spectra represent the pre-atmospheric-entry distribution of PAHs and that the higher degrees of alky-

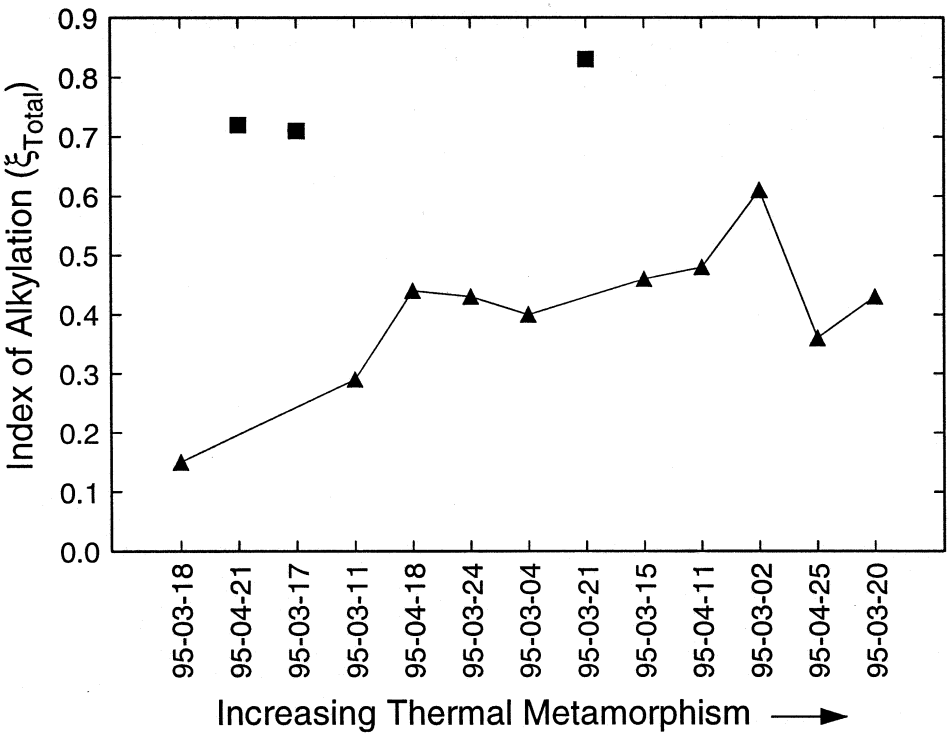

Figure 7. Correlation plot of the index of alkylation, ξ, for AMMs versus thermal metamorphism as determined by the degree of vesicle invasion. The three particles lying well above the solid line represent the three non-CM-type AMMs illustrated in Figure 1b.

lation observed in the more highly metamorphosed particles are a consequence of atmospheric heating. If this hypothesis is correct, then it is also likely that the pre-atmospheric-entry PAH content of AMMs is larger than that of carbonaceous chondrites like Murchison (CM2). In this regard, the yields of the residual PAHs observed in the most strongly depleted mass range, 78 to 178 amu, still show a value similar to or even higher than in Murchison in about 40% of the dehydrated AMMs. It is possible that future simulation experiments into the effects of thermal processing using a homogenized Murchison (CM2) matrix will help in assessing the 'equivalent' temperature of thermal metamorphism suffered by CM-type AMMs during atmospheric entry.

4.3. Search for correlation between PAHs and major and minor element compositions

In the Figure 2 upper panel we reported the accurate electron microprobe analyses of the fifteen AMMs investigated in this work. The ternary Si/Mg/Fe diagram indicates that all particles lie in the region of so-called chondritic composition

previously defined from the detailed analyses of several hundreds AMMs. No specific clustering of the particles with high ξ values are observed.

The electron microprobe data can be used to generate correlation plots to search for possible relationships between the values of the total desorption yield, γ_{Total}, and/or alkylation index, ξ, with various diagnostic element/Si ratios. The only significant correlation is observed between ξ_{Total} and the Na/Si ratio, which is illustrated in Figure 8, where the four highest ξ_{Total} values cluster in the region with the highest Na/Si ratios. From this observation it appears that the parent body of IDPs and some of the high ξ AMMs were somewhat enriched in Na, an element considered as very mobile during either aqueous alteration or thermal metamorphism.

5. Conclusions and Future Prospects

Studies of the mineralogy, chemistry, and isotopic composition of AMMs indicate that they are related to carbonaceous chondrites. In spite of these similarities, major differences also exist between these two classes of Solar System objects. AMMs show a higher C content, a pyroxene to olivine ratio $\sim$10 times higher than of the carbonaceous chondrites, and a marked absence of chondrules [11].

With regard to comparisons between carbonaceous chondrites and ordinary chondrites the traditional view in meteoritics is that either an increase in C or an absence of chondrules indicates that the parent body of a given meteorite formed at a larger heliocentric distance [11]. As this trend is sharply enhanced in large micrometeorites, it seems likely they are samples from bodies formed at even larger heliocentric distances than are the chondrites. Hence AMMs represent a new population of Solar System objects not present in current meteorite collections.

There are also similarities and differences specifically between the PAH distributions observed in AMMs and Murchison (CM2) that further support this conclusion. Similarities include the observation that three of the major peaks in the micrometeorite PAH spectra (178, 202 and 228 amu) are also observed as dominant peaks in the spectra of the carbonaceous chondrites and that the total integrated PAH yields stay within the range bracketed by the lowest and highest values observed for Orgueil (CI1) and Allende (CV3) chondrites, respectively.

In regard to differences, the 10 CM-type AMMs (five of which show vesicle invasion) have consistently higher desorption yields, γ, than Murchison (CM2). Moreover, the extent of aromatization is generally higher in AMMs, as is the degree of alkylation, ξ. Finally, the presence of strong peaks consistent with vinyl-PAHs have so far only been observed in AMMs.

Although more work is clearly necessary before it can be established beyond statistical error that these differences directly reflect origins with a different set of parent bodies formed at a larger heliocentric distance, this hypothesis seems to account for our observations.

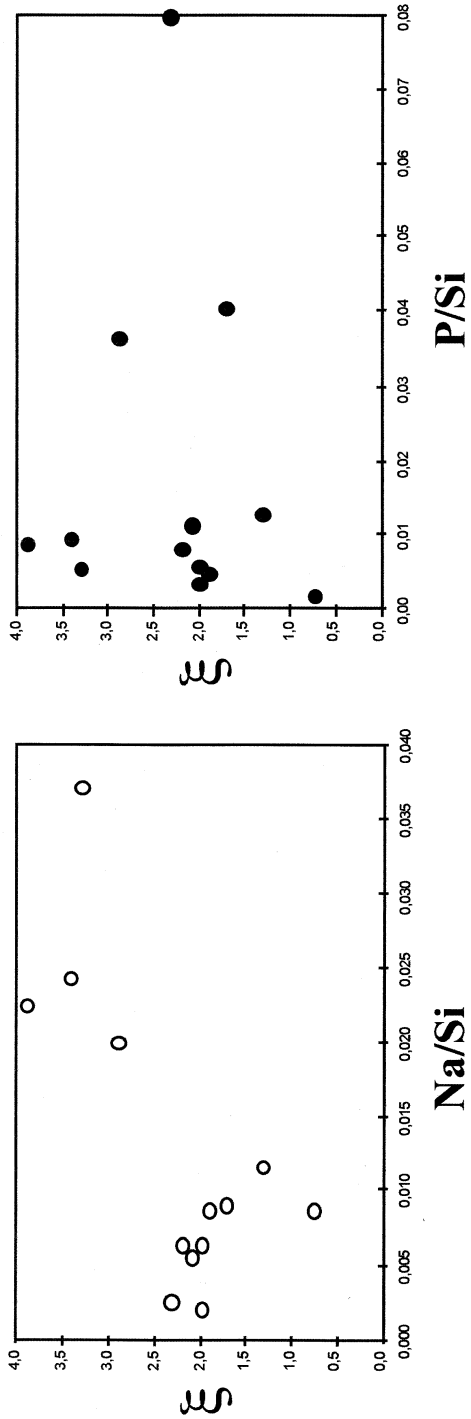

Figure 8. Correlation plots between the values of the index of alkylation, ξ, and the Na/Si and P/Si ratios.

The mass flux of micrometeorites accreted by the Earth is far greater than that of macroscopic carbonaceous meteorites. It is estimated by us that AMMs deliver about 30 000 times the quantity of PAHs to the Earth than do carbonaceous chondrites. Also the PAHs delivered by AMMs include a much richer variety of molecules, including highly alkylated PAHs and chemically reactive vinyl-PAHs.

Shock and Schulte [35] have suggested that PAHs might have been involved in the synthesis of complex organic molecules such as amino acids in meteorites by a mechanism of catalyzed hydrolysis operating during aqueous alteration on the meteorite parent bodies. This mechanism may have also been effective on the early Earth, as soon as carbonaceous micrometeorites came in contact with water. Because the variety and chemical reactivity of the micrometeorite PAHs is much larger than in meteorites, this mechanism should have been even more efficient with micrometeorites, especially those containing vinyl-PAHs. In this regard, micrometeorites of the CM-type, belonging to the dominant mass fraction captured by the Earth today, should have played a significant role in the synthesis of prebiotic molecules on the early Earth [11].

Acknowledgements

This work was supported in the USA by NASA grant NAGW-3629, and in France by 'Programme d'Exobiologie' of the French Space Agency (CNES). Stimulating comments by A. Brack, L. d'Hendrecourt and S. Leach were appreciated.

References

1. Hahn, J. H., Zenobi, R., Bada, J. F. and Zare, R. N.: 1988, *Science* **239**, 1523.
2. Zenobi, R., Philippoz, J.-M., Buseck, P. R. and Zare, R. N.: 1989, *Science* **246**, 1026.
3. Zenobi, R., Philippoz, J.-M., Zare, R. N., Wing, M. R., Bada, J. L. and Marti, K.: 1992, *Geochim. Cosmochim. Acta* **56**, 2899.
4. McKay, D. S., E. K. G. Jr., Thomas-Keprta, K. L., Vali, H., Romanek, C. S., Clemett, S. J., Chillier, X. D. F., Maechling, C. R. and Zare, R. N.: 1996, *Science* **273**, 924.
5. Kovalenko, L. J., Maechling, C. R., Clemett, S. J., Phillipoz, J.-M., Zare, R. N. and Alexander, C. M. O. D.: 1992, *Anal. Chem.* **64**, 682.
6. Clemett, S. J., Maechling, C. R., Zare, R. N., Swan, P. D. and Walker, R. M.: 1993, *Science* **262**, 721.
7. Thomas, K. L., Blanford, G. E., Clemett, S. J., Flynn, G. J., Keller, L. P., Klock, W., Maechling, C. R., Mckay, D. S., Messenger, S., Nier, A. O., Schlutter, D. J., Sutton, S. R., Warren, J. L. and Zare, R. N.: 1995, *Geochimica et Cosmochemica Acta* **59**, 2797.
8. Clemett, S. J.: 1996, 'Laser Microprobe Studies of Complex Aromatic Hydrocarbons on Meteorites and Interplanetary Dust Particles', Ph.D Thesis, Stanford University.
9. Whipple, F. L.: 1951, *Proc. N.A.S., USA* **37**, 19.
10. Love, S. G. and Brownlee, D. E.: 1991, *Icarus* **89**, 26.
11. Maurette, M.: 1996, 'Carbonaceous Micrometeorites and the Origin of Life', *Proc. 11th Int. Conf. Origin of Life* (in press).
12. Engrand, C., Michel-Levy, M. C., Jouret, C., Kurat, G., Maurette, M. and Perreau, M.: 1994, *Meteoritics* **29**, 464.

13. Maurette, M., Bonny, P., Brack, A., Jouret, C., Pourchet, M. and Siry, P.: 1991, *Lecture Notes in Physics* **390**, 124.
14. Hammer, C. and Maurette, M.: 1996, *Meteoritics* **31**, A56.
15. Love, S. G. and Brownlee, D. E.: 1993, *Science* **262**, 550.
16. Brownlee, D. E.: 1985, *Ann. Rev. Earth Planet. Sci.* **13**, 147.
17. Brinton, K. L., Engrand, C., Bada, G. and Maurette, M.: 1996, 'The Search for Amino Acids in 'Giant' Carbonaceous Micrometeorites from Antarctica', *Proc. 11th Int. Conf. Origin Life* (in press).
18. Maurette, M., Brack, A., Kurat, G., Perreau, M. and Engrand, C.: 1995 *Adv. Space Res.* **15**, 113.
19. Maurette, M., Immel, G., Hammer, C., Harvey, R., Kurat, G. and Taylor, S.: 1994, 'Collection and Curation of IDPs from the Greenland and Antarctic Ice Sheets', in Zolensky, M. E., Wilson, T. L., Rietmeijer F. J. M. and Flynn, G. (eds.), *Analysis of Interplanetary Dust*, New York: Amer. Inst. Physics, pp. 277–289.
20. Maechling, C. R., Clemett, S. J., Engelke, F. and Zare, R. N.: 1996, *J. Chem. Phys.* **104**, 8768.
21. Pappas, D. L., Hrubowchak, D. M., Ervin, M. H. and Winograd, N.: 1989, *Science* **243**, 64.
22. Winograd, N., Baxter, J. P. and Kimock, F. M.: 1982, *Chem. Phys. Lett.* **82**, 581.
23. Shibanov, A. N.: 1985, *Laser Analytical Spectrochemistry*: Adam Hilger, Bristol.
24. Zenobi, R. and Zare, R. N.: 1991, 'Two-Step Laser Mass Spectrometry', in Lin, S. H. (ed.), *Advances in Multiphoton Processes and Spectroscopy*, **7**, Singapore: World Scientific, pp. 1–167.
25. Zolensky, M. and McSween, J. H. Y.: 1988, 'Aqueous Alteration', in Kerridge, J. F. and Matthews, M. S. (eds.), *Meteorites and the Early Solar System, Space Science Series*, Tuscon: The University of Arizona Press, pp. 114–143.
26. McSween, H. Y., Sears, D. W. G. and Dodd, R. T.: 1988, 'Thermal Metamorphism', in Kerridge, J. F. and Matthews, M. S. (eds.), *Meteorites and the Early Solar System, Space Science Series*, Tuscon: The University of Arizona Press, pp. 102–114.
27. Brack, A.: 1996, 'Why Exobiology on Mars', *Planet. Space Sci.* (in press).
28. Clemett, S. J., Messenger, S., Chillier, X. D. F., Gao, X., Walker, R. M. and Zare, R. N.: 1996, 'Indigenious Polycyclic Aromatic Hydrocarbon Molecules in Circumstellar Graphite Grains', *Lunar and Planetary Science XXVII*, pp. 229–230.
29. v. Schmus, W. R. and Wood, J. A.: 1967, *Geochimica et Cosmochimica Acta*, **31**, 747.
30. McSween, H. Y.: 1979, *Rev. Geophys. Space Phys.* **17**, 1059.
31. Sears, D. W. G. and Dodd, R. T.: 1988, 'Overview and Classification of Meteorites', in Kerridge, J. F. and Matthews, M. S. (eds.), *Meteorites and the Early Solar System, Space Science Series*, Tuscon: The University of Arizona Press, pp. 3–31.
32. Flynn, G. J.: 1995, 'Chemical Composition of Large Stratospheric Dust Particles: Composition of Large Stratospheric Dust Particles: Comparison with Stratospheric IDPs, Cluster Fragments, and Polar Micrometeorites', *Lunar and Planetary Science XXVI*, pp. 407–408.
33. Flynn, G. J.: 1995, 'Thermal Gradients in Interplanetary Dust Particles: The Effect of an Endothermic Phase Transition', *Lunar and Planetary Science XXVI*, pp. 405–406.
34. Engrand, C., Deloule, E., Maurette, M., Kurat, G. and Robert, F.: 1996, *Meteoritics* **31**, A43.
35. Shock, E. L. and Schulte, M. D.: 1990, *Nature* **343**, 728.